# Supplementary Information

## Turn-on fluorescence detection of protein by molecularly imprinted hydrogels based on supramolecular assembly of peptide multifunctional blocks

Battista Edmondo[1], Scognamiglio P. Liana[2], Di Luise Nunzia[2], Raucci Umberto[3], Donati Greta[3], Rega Nadia[3], Netti Paolo Antonio[1,2,4] and Causa Filippo[1,2,4].

[1)] Interdisciplinary Research Centre on Biomaterials (CRIB) Università degli studi di Napoli "Federico II", Piazzale Tecchio 80, 80125, Napoli, Italy;

[2)] Center for Advanced Biomaterials for HealthCare@CRIB, Istituto Italiano di Tecnologia, Largo Barsanti e Matteucci 53 80125 Napoli, Italy;

[3)] Dipartimento di Scienze Chimiche, Università degli studi di Napoli "Federico II", Complesso Universitario di M.S.Angelo, via Cintia, I-80126, Napoli, Italy;

[4)] Dipartimento di Ingegneria Chimica, dei Materiali e della Produzione Industriale (DICMAPI), Università degli studi di Napoli "Federico II", Piazzale Tecchio 80, 80125, Napoli, Italy;

Corresponding author: Filippo Causa, email: causa@unina.it

## SUPPLEMENTARY EXPERIMENTAL SECTION

### Set up for HydroMIP preparation

We varied the concentration of monomers and cross-linker and for simplicity these changes were reported as function of two parameters: the total monomer concentration (T %) and the cross-linking density (C %), defined as follows:

$$T\,\% = \sum \%monomers$$

$$C\,\% = \frac{\%\,Crosslinking}{T\%} * 100$$

As for polyacrylamide gels in protein separation (PAGE), the pore size can be tuned by changing the T% and C% values. It is well known that these parameters influence the mesh size of gel polymer matrix and can be utilized for HydroMIP formulations. In particular, in the imprinting of small molecules, a high crosslinking density (C>70%) is required in order to reduce the swelling and maintain the stability of the recognition cavities. However, this rule is not suitable for the imprinting of proteins because small pore size of highly cross-linked polymers would limit their free diffusion through the polymer network. With increasing T%, the pore size decreases in a nearly linear relationship. The relationship of C% to pore size is more complex. Generally, decreasing C% results in a more open pore structure, because there are fewer cross-linker molecules. Increasing C% also can increase the pore size, because of nonhomogeneous bundling of strands in the gel. Overall, this situation is reflected on the binding features of the imprinted hydrogels [1] [2] [3].

Here equilibrium-binding studies of a dye-labeled template (BSA-FITC) were performed to compare the performances of the HydroMIPs. Fluorescence confocal microscopy was adopted to assess the amount of BSA-FITC allowing for a direct and micro-scale observation of the uptake within the polymer matrix of particles of comparable size.

For a fast screening of the formulation, we define three parameters to be assessed as follow:

- binding capacity of BSA-FITC at a defined concentration to the HydroMIPs.

- imprinting ratio, defined as the amount of ligand emitting fluorescence BSA-FITC bound to the HydroMIP over the HydroNIP (Non-imprinted polymer)[4], according to the following expression:

$$IR\,(HydroMIP/HydroNIP) = \frac{Fluo_{HydroMIP}}{Fluo_{HydroNIP}}$$

- selectivity of the binding (S) of the template over an interfering protein (lysozyme). The selectivity is defined by displacement experiments where an excess of interfering protein competitor (BSA or lysozyme, LYS) compete for the binding of BSA-FITC to the HydroMIPs[4] and reported as follow:

$$S = \frac{Fluo_{HydroMIP\ BSA-FITC+BSA}}{Fluo_{HydroMIP\ BSA-FITC+LYS}}$$

**Polymer Characterization**

***Microparticles size***

The size of the polymers was estimated by laser diffraction method (Mastersizer S, Malvern Instruments Limited). The dried microparticles, dispersed in PBS 0.01 M, were measured after 90 s of sonication to prevent aggregation before measurement. Samples were analyzed in triplicate. The particle size was expressed as the mean volume diameter in µm.

***SEM analysis and FT-IR***

SEM analysis was performed by an FE-SEM ZEISS ULTRAPlus operating at 10 kV by using secondary electron as detector. The polymer was deposited on a holder and dried at room temperature; then, this sample was sputter coated by 10 nm of gold (Cressingthon Sputter Coater, HR208). After homogenization polymer assumes the typical multifaceted shape of crushed particles with size around 130 µm.

FTIR spectra were taken on a Nicolet 7600 FTIR ThermoFisher by accumulating 64 scan with a spacing of 8 $cm^{-1}$. The spectra of the polymers showed the amide bands centered around 1650 and 1550 $cm^{-1}$ typical of acrylamide and proteins.

***Template removal***

Once terminated the polymerization, the monolithic gel was collected in a beaker, 90 mL PBS were added and a homogenization cycle of 15 min produced sub-150 µm particles. The resultant microparticles were transferred in 50 mL conical tubes, collected by centrifugation at 4500 rpm for 10 min and washed repeatedly to remove the protein template, adsorbed oligomers and unreacted monomers. In particular, the polymers were washed four times with PBS buffer, followed by four rinses with NaOH 1M/PBS and four rinses more in water. The “wash cycle 0” represents the measurement done soon after the homogenization step. In this case the burst we observed might be attributed to the huge amount of protein squeezed out occurring during the crushing step. (Fig. S1a and b).

To validate the washing procedures, samples from each rinse were analyzed for residual BSA identification via UV spectroscopy at 280 nm. Briefly, after the addition of a known volume of a desired wash solution, the samples were placed on a rotating mixer for 20 min to allow adequate time for diffusion, and centrifuged for 10 min (4500 rpm); then the supernatant was analyzed through UV/VIS instrument. The time for diffusion was chosen by taking in account the diffusion coefficient of BSA in water at 20°C ($5.9 \cdot 10^{-7}$ $cm^2/sec$) and the microparticles diameter previously determined. The amount of BSA removed at step *i* was calculated by equation:

$$M_i = (V * C)^{MIP} - (V * C)^{NIP}$$

Where M is the BSA mass removed in step *i*, V is the volume of supernatant decanted in step *i* and C is the protein concentration determined from absorbance measurement using Lambert-Beer equation. All spectra were subtracted with the spectrum recorded from monomers solution. The mass removed in each step was summed to yield the total mass removed, which was then rationed to the total amount of BSA added in the synthesis (Fig. S1b).

**Active Assistant Recognition Elements (AAREs) Design and Synthesis**

The active assistant recognition elements (AARE) are peptides designed and synthesized starting from the following sequences: -EDICLPRWGCLWEDD- (serum albumin peptide, SAp) as positive control and the -EGGCGGRGGCGGEDD- (peptide as negative control, SActrl) as unrelated sequence, used in the control experiments. SAp was previously selected by phage display toward serum albumin[5] and has a 5 residues recognition sequence within a cycle formed through a disulfide bridge $Cys^4$-$Cys^{10}$.

Single peptides were prepared by the solid phase method on a 75 μmol scale following the Fmoc strategy and using standard Fmoc-derivatized amino acids. Briefly, synthesis was performed on a fully automated multichannel peptide synthesizer Biotage Syro Wave (Biotage, SW). Rink amide resin (substitution 0.71 mmol/g) was used as solid support. Activation of amino acids was achieved using HBTU-HOBt-DIPEA (1:1:2), whereas Fmoc deprotection was carried out using a 40% (v/v) piperidine solution in DMF. All couplings were performed for 15 minutes and deprotections for 10 minutes. The allyl group at C-terminus was incorporated as Fmoc-Asp(Oallyl)-OH and spaced from the active core sequence by a Fmoc-βAla-OH. At N-terminus, after the sequential addition of two residues of Fmoc-βAla-OH, the dansyl group has been introduced using the modified amino acid Fmoc-Lys(dansyl)-OH. The acetylation of the N-terminal was achieved using a solution of acetic anhydride (20%) and DIPEA (5%) in DMF for 15 mins. Peptides were removed from the resin by treatment with a TFA:TIS:$H_2O$ (90:5:5, v/v/v) mixture, then they were precipitated in cold diethylether and lyophilized. The purification and characterization of the peptides were performed

by high performance liquid chromatography techniques (HPLC). Single peptides were purified by preparative reversed-phase high performance liquid chromatography (RP-HPLC) using a Waters 2535 Quaternary Gradient Module, equipped with a 2489 UV/Visible detector and with an X-Bridge BEH300 preparative 10× 100 mm C8, 5μm column and applying a linear gradient of 0.1% TFA/$CH_3CN$ in 0.1% TFA/water from 5% to 60% over 25 min. Following, peptides purity and identity were confirmed by liquid chromatography mass-spectrometry (HPLC-MS) analyses on an Agilent 6530 Accurate-Mass Q-TOF LC/MS spectrometer. Zorbax RRHD Eclipse Plus C18 2.1 x 50 mm, 1.8 μm column was used for these analyses. After peptide purification, single peptide was dissolved in carbonate buffer pH=9 and cyclized by air oxidation for 1 day to form the disulfide bridge. NMR spectra were recorded using an Agilent 600MHz (14 Tesla) spectrometer equipped with a DD2 console and an OneNMR HX probe. The AARE sequence (1mg) was dissolved in 600μL of $H_2O$:$D_2O$ (90:10) solution. $^1H$ 1D , 2D TOCSY and 2D NOESY spectra were recorded at 300 K°. 2D TOCSY and 2D NOESY experiments were recorded with a mixing time of 80ms and 300ms respectively. Spectra were transformed and analyzed using VNMRJ 4 and CCP_Analysis (http://www.ccpn.ac.uk/v2-software/software/analysis) software. Chemical shift scale was referenced on the water residual peak signal.

**SAp and AAREs Characterizations and Affinity binding evaluation**

***Isothermal Titration Calorimetry analysis***

The binding affinity parameters between peptides and BSA were obtained by Isothermal Titration Calorimetry (ITC), (nano-ITC low-volume calorimeter, TA Instruments). The SAp sequence (Fig. S7a and b) or AARE (Fig. 1c) dissolved in PBS at a concentration of 1 mM was injected into the cell containing a BSA solution (0.1 mM). The stepwise experiments were conducted with 25 aliquots of 2 μL of peptide solution injected with 200 s intervals. Heat produced by peptide or BSA dilutions was evaluated by performing a control experiment, titrating the peptide into the buffer alone. The interaction heat for each injection was calculated after correction for the heat coming from molecules dilution. The resulting corrected injection heats were plotted as a function of the weight ratio between peptide and protein concentrations, fitted with a model for one set of binding sites and analyzed with a nonlinear least-squares minimization algorithm, using the program NanoAnalyze software, version 2.4.1 (TA Instruments). The unrelated sequence was used in a control experiment (Fig. S7c).

***Surface Plasmon Resonance analysis***

The SensiQ Pioneer SPR system for Real Time kinetic analysis was from SensiQ (USA). BSA was diluted in 10 mM acetate buffer pH 3.7 and immobilized on a COOH5 sensor chip, using EDC/NHS chemistry (flow rate= 5 μL/min, time injection= 7 min). Residual reactive groups were deactivated by treatment with 1 M ethanolamine hydrochloride, pH 8.5. References channels were prepared simply activating with EDC/NHS and deactivating with ethanolamine. Affinities SPR experiments were carried out incubating the SAp sequence at different concentrations (injections of 90 μL at a flow rate of 20 μL/min), ranging from 1 μM to 250 μM. The bound peptide was allowed to dissociate for 5 min, before surface regeneration using 10 mM glycine, pH 3.0. All sensorgrams were subtracted with signals from injections passing on the reference cell. The Qdat software was used to determinate $K_D$ from the association and dissociation rates using a one-to-one binding model.

***Steady-state and lifetime fluorescence***

Fluorescence emission spectra and lifetime values of the AARE sequences and their complexes with BSA were collected in a quartz cell using a spectrofluorometer (FluoroMax-4 Horiba Scientific). The spectra were recorded in PBS (pH 7.4 0.01 M) by exciting at 340 nm and collecting emission between 400 and 630 nm with 5 nm bandpass. The AARE solution (1 μM) was titrated by dropping 0.8 μL aliquots of BSA solution (100 μM). The same experiment was carried out with the n-AARE peptide.

Fluorescence lifetimes were recorded with a time-correlated single photon counting (TCSPC) system (FluoroMax-4 Horiba Scientific), exciting with a pulsed laser diode (320 nm, 60 ps pulse duration). Lifetime traces were recorded with the monochromator at 500 nm, 8-nm slit width, and a collection time of 10,000 counts in the peak channel. The instrument response was recorded using scattering solutions (LUDOX) at 320 nm. Data was fitted to a sum of exponential decays using iterative deconvolution in the DAS6 decay analysis software.

**Binding Studies by Microfluorimetry**

Batch re-binding tests were realized to study the affinity of the hybrid imprinted polymers by using microfluorimetry on a confocal laser-scanning microscope. A fluorescent-conjugated template (albumin fluorescein isothiocyanate conjugate, FITC-BSA) was used to directly visualize the adsorption in the polymer matrix. Images and z-sections of polymers were collected by a CLSM Leica TCS SP5, using argon laser line 488 nm, objective 40.0x1.10 water, pinhole XX AU (estimated of section thickness 3.50 μm), scan speed 400 Hz, λ em range 500-550 nm. For the

equilibrium binding studies, a known amount of freeze-dried polymer (5 mg) of a specific formulation was dissolved in 0.5 mL of PBS (0.01 M pH 7.4,) and placed on a rotating mixer for 1 h to allow swelling. Then, 0.5 mL of FITC-BSA solutions at different concentrations were added to the suspension including polymer gel particles to give final FITC-BSA concentrations in the range 0.01-2.25 μM. Samples were placed in a rotating mixer and allow for equilibrating for 2 hours at 25°C. Once reached the equilibrium, 0.02 mL of the polymer solution was deposited on a cover glass for microscopy analysis. Five images were collected for each sample. By analyzing fluorescent intensity values from polymer microparticles of similar size, quantitative analysis of FITC-BSA amount bound to the network were obtained. All captured images were analyzed with a public domain image-processing Image J.

**Selectivity studies by Microfluorimetry**

Selectivity of imprinted polymers was performed by microfluorimetry on a confocal laser-scanning microscope by competition assays between FITC-BSA and three different non fluorescent proteins. Lysozyme (LYS, MW ~14.5 kDa, pI 11.3, Rh , Rg , 45 × 30 × 30 Å) and Ovalbumin (OVA, MW ~44.3 kDa, pI 4.5, 70 × 36 × 30 Å, Rh nm) were chosen as competitor proteins. The template, Bovine Serum Albumin (BSA, MW ~65 kDa, pI 4.9, 75 × 65 × 40 Å, Rh nm) was also tested. Briefly, a known amount of freeze-dried polymer (5 mg) of a specific formulation was dissolved in 0.2 mL of PBS (0.01 M, pH 7.4) and placed on a rotating mixer for 20 min to allow swelling. Then, 0.4 mL of FITC-BSA solution (0.075 μM) was added to 0.4 ml of competitor protein solutions at different concentrations to give different FITC-BSA:competitor protein molar ratio (1:0, 1:100, 1:300). After, this protein mixture was added to the polymer suspension. The samples were placed in a rotating mixer and allowed to equilibrate for 2 hours. Once reached the equilibrium, an aliquot (0.02 mL) of the suspension including polymer gel particles was collected and analyzed to the microscope, as previously described.

**Steady-state and lifetime fluorescence studies for BSA/Dansyl-HyPPIs interaction**

Fluorescence emission spectra and lifetime values of Dansyl-HyPPIs and in complex with BSA were collected in a quartz cell using a spectrofluorometer (FluoroMax-4 Horiba Scientific). The spectra were recorded in PBS (pH 7.4 0.01 M) by exciting at 340 nm and collecting emission between 390 and 590 nm with 5 nm bandpass. A Dansyl-HyPPI suspension (0.5 mg/mL) was titrated by dropping 0.8 μL aliquots of BSA solution from a stock solution of 100 μM, under stirring.

Fluorescence lifetimes were recorded with a time-correlated single photon counting (TCSPC) system (FluoroMax-4 Horiba Scientific), exciting with a pulsed laser diode (320 nm, 60 ps pulse

duration). Lifetime traces were recorded with the monochromator at 440 nm, 8-nm slit width, and collection time of 10,000 counts in the peak channel. The instrument response was recorded using scattering solutions (glycogen 0.1%) at 320 nm. Data was fitted to a sum of exponential decays using iterative deconvolution in the DAS6 decay analysis software.

## SUPPLEMENTARY TABLES

### Set up for HydroMIP preparation

**Table S1 –** In the table is reported the recipe of poly-acrylamide-co-acrylic acid hydrogel networks cross-linked by bis-acrylamide (BIS) expressed as molar W/V percentage. T% and C% are defined respectively as total monomer concentration and cross-linking density. Binding parameters are expressed in fluorescence intensity emission of BSA-FITC in arbitrary units taken at same instrumental conditions inside the polymer matrix. Displacement of BSA-FITC is referred to the selectivity experiments, where the residual fluorescence intensity is measured inside the polymer after competitive adsorption of BSA and Lysozyme.

| | | | | Binding of BSA-FITC | | | Displacement of BSA-FITC | | |
|---|---|---|---|---|---|---|---|---|---|
| Aam (%) | Aac (%) | Bis (%) | T%:C% | HydroMIP | HydroNIP | IR (HydroMIP/ HydroNIP) | HydroMIP + BSA | HydroMIP + LYS | Selectivity ($HydroMIP_{BSA}$/ $HydroMIP_{LYS}$) |
| 9 | 4,5 | 0,5 | 14%T:3.6%C | 480 | 350 | 1,37 | 325 | 180 | 0,55 |
| 6 | 3 | 0,5 | 9.5%T:5.3%C | 470 | 300 | 1,57 | 310 | 200 | 0,65 |
| 3 | 1,5 | 0,5 | 5%T:10%C | 380 | 180 | 2,11 | 250 | 230 | 0,92 |
| 9 | 4,5 | 1 | 14.5%T:6.9%C | 350 | 250 | 1,40 | 280 | 195 | 0,70 |
| 6 | 3 | 1 | 10%T:10%C | 550 | 190 | 2,89 | 380 | 215 | 0,57 |
| 3 | 1,5 | 1 | 5.5%T:18.2%C | 600 | 265 | 2,26 | 350 | 230 | 0,66 |
| **9** | **4,5** | **1,5** | **15%T:10%C** | **580** | **150** | **3,87** | **330** | **450** | **1,36** |
| 6 | 3 | 1,5 | 10.5%T:14.3%C | 450 | 135 | 3,33 | 320 | 380 | 1,19 |
| 3 | 1,5 | 1,5 | 6%T:25%C | 250 | 97 | 2,58 | 180 | 200 | 1,11 |
| 9 | 4,5 | 3 | 16.5%T:18.18% C | 187 | 150 | 1,25 | 150 | 120 | 0,80 |
| 6 | 3 | 3 | 12%T:25%C | 210 | 97 | 2,16 | 170 | 150 | 0,88 |
| 3 | 1,5 | 3 | 7.5%T:40%C | 315 | 75 | 4,20 | 220 | 198 | 0,90 |

**Table S2.** Peptide and AARE sequences. Amino acids in bold indicate those of the core sequence, whereas the underlined involved in a disulphide bridge.

| | |
|---|---|
| **SAp** | **E**DIC<u></u>LPRWGC<u></u>LW**EDD** |
| **SAp-Oall** | E**DIC<u></u>LPRWGC<u></u>LW**EDD-βA-D(Oall) |
| **AARE** | K-dansyl-βAβA-E**DIC<u></u>LPRWGC<u></u>LW**EDD-βA-D(Oall) |
| **n-AARE** | K-dansyl-βAβA-EGG**C<u></u>**GG**R**G**GC<u></u>**GGEDD-βA-D(Oall) |

**Table S3.** Lifetime values of AARE and the corresponding control in solution.

| | **BSA ratio** | **τ1** | **fraction 1** | **τ2** | **fraction 2** | **τ average** |
|---|---|---|---|---|---|---|
| AARE | 0 | 4.2 | 0.64 | 11.6 | 0.36 | 8.7 |
| | 0,5 | 4.5 | 0.62 | 15.0 | 0.38 | 11.6 |
| | 1 | 4.6 | 0.65 | 16.6 | 0.35 | 12.5 |
| n-AARE | 0 | 4.2 | 0.88 | 15.9 | 0.12 | 8.2 |
| | 0,5 | 4.12 | 0.87 | 15.6 | 0.13 | 8.3 |
| | 1 | 4.2 | 0.86 | 15.9 | 0.14 | 8.7 |

## SUPPLEMENTARY FIGURES

### Template removal Step

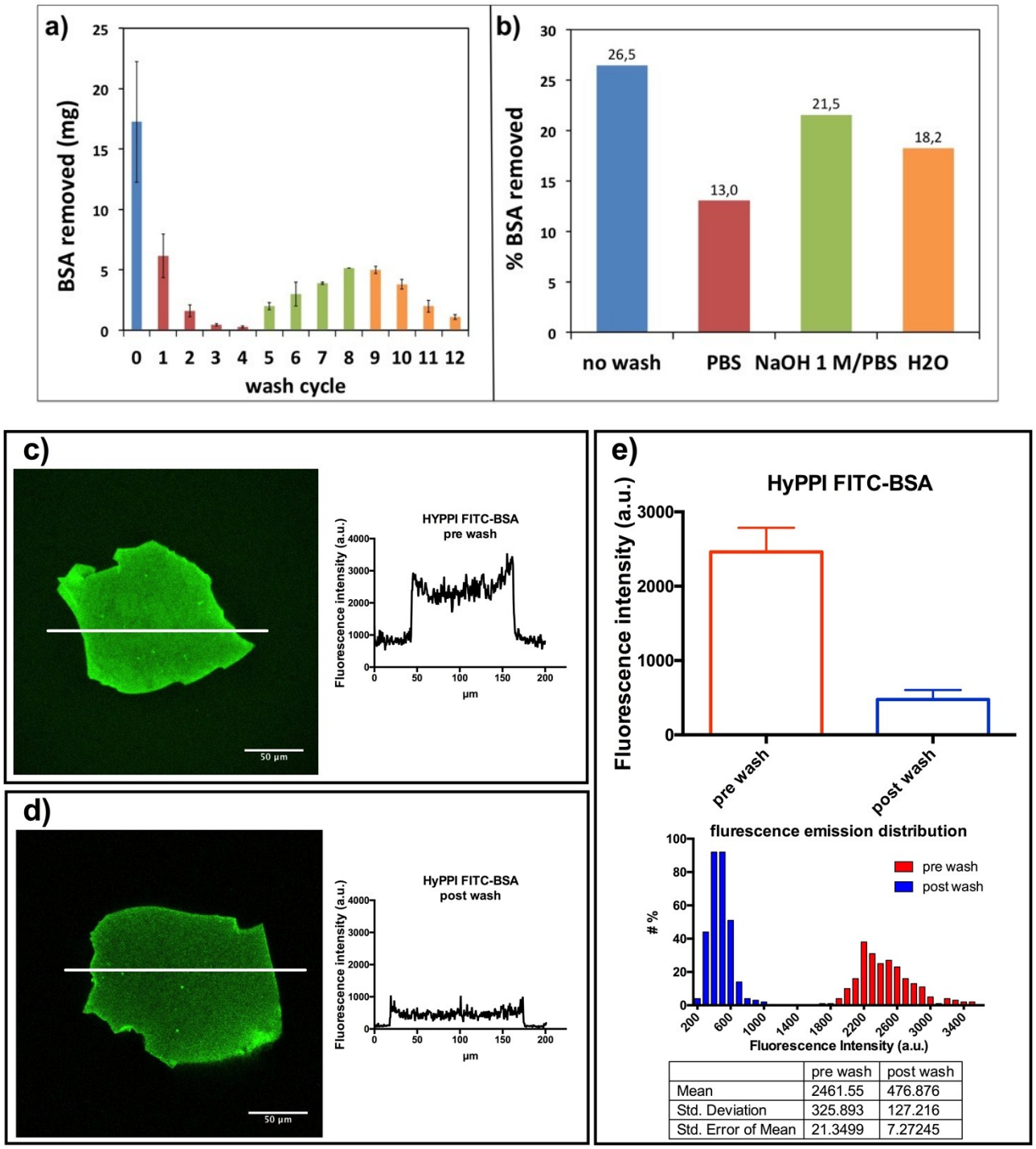


| | pre wash | post wash |
|---|---|---|
| Mean | 2461.55 | 476.876 |
| Std. Deviation | 325.893 | 127.216 |
| Std. Error of Mean | 21.3499 | 7.27245 |

**Fig. S1:** Histograms reporting a) mass of BSA removed at each wash cycle measured in solution and b) % BSA removed with each washing solution. c) and d) Template removal steps monitored on HyPPI by microfluorimetry realized by imprinting FITC-BSA (15%T:10%C) and imaged by CLSM. Plot profiles were taken across the imprinted particles and averaged. e) The template removal efficiency is calculated averaging the emission from a line drawn across polymer particles; the washing efficiency directly measured inside the polymer particles was around 80%.

**FT-IR Data**

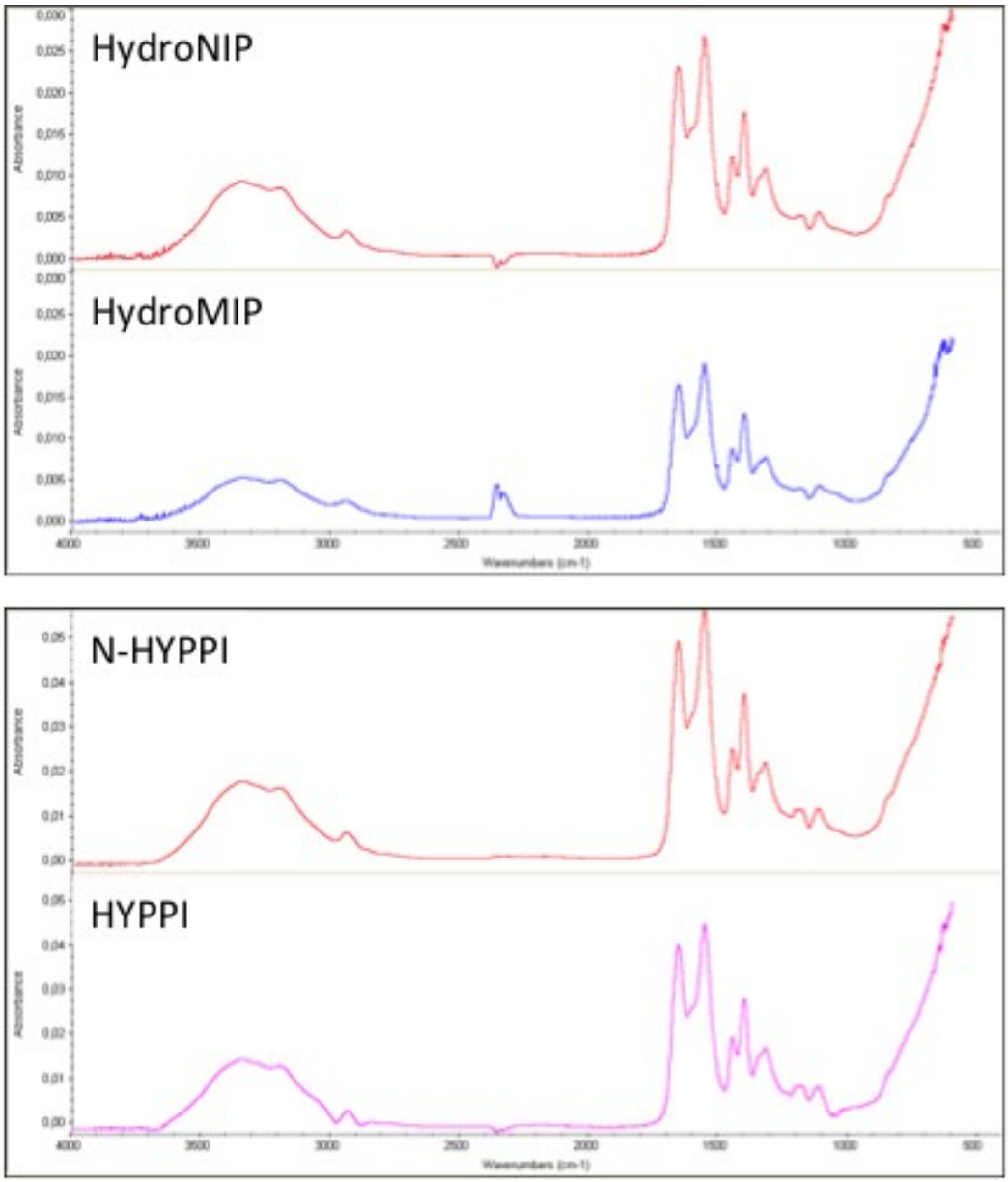


**Fig. S2:** FT-IR spectra of imprinted and not-imprinted polymers.

**Master Sizer Data**

HydroMIP

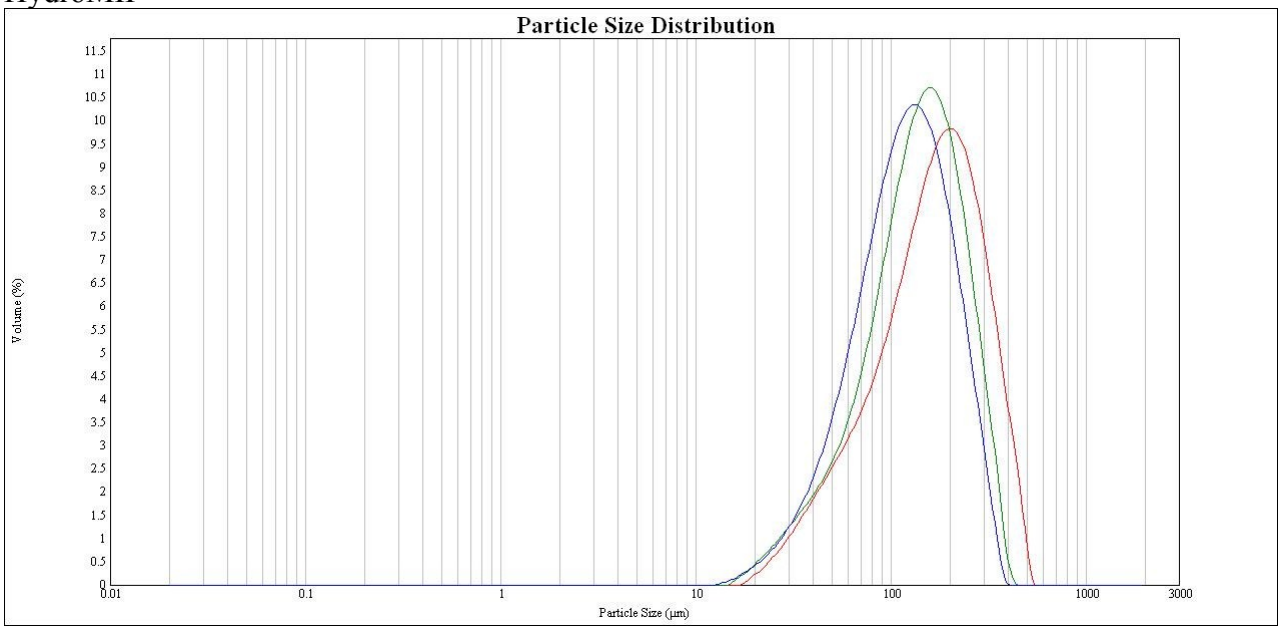


HydroNIP

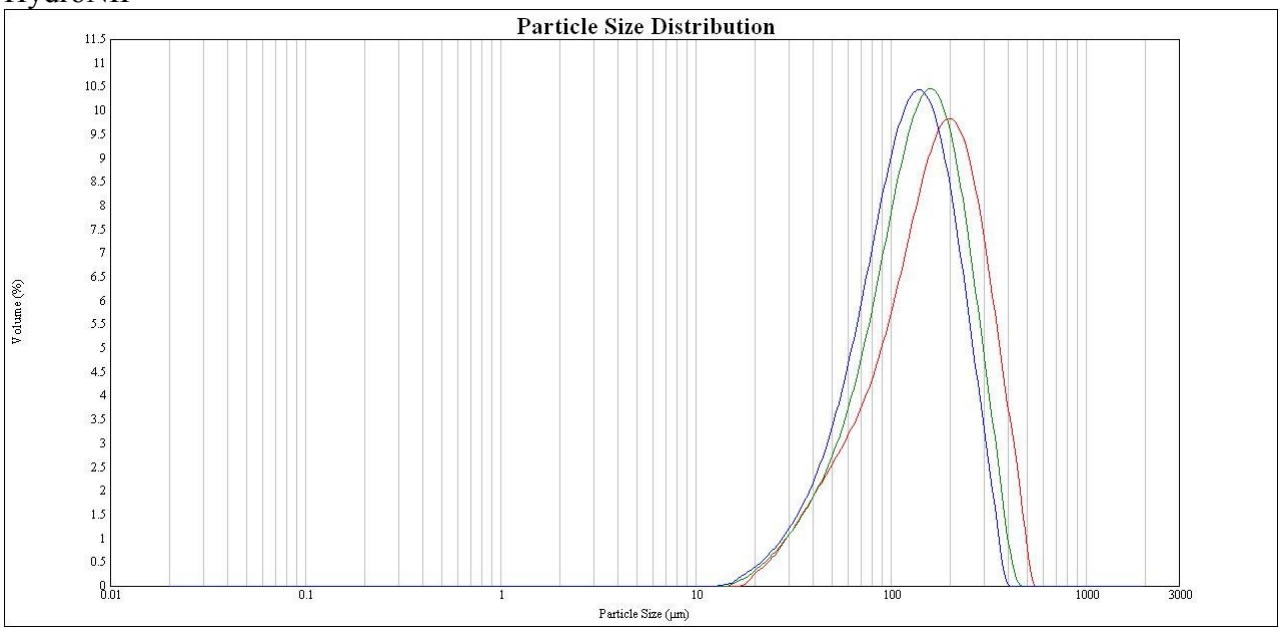


| Sample particles | TIME OF HOMOGENIZER (MIN) | | |
|---|---|---|---|
| | 5 | 10 | 15 |
| HydroMIP | 182.07 µm | 149.62 µm | 131.50 µm |
| HydroNIP | 181.10 µm | 151.92 µm | 135.73 µm |

**Fig. S3:** Comminution of bulk hydrogels by homogenizer brings to particles in the range of 130-180 µm.

**SEM Analysis**

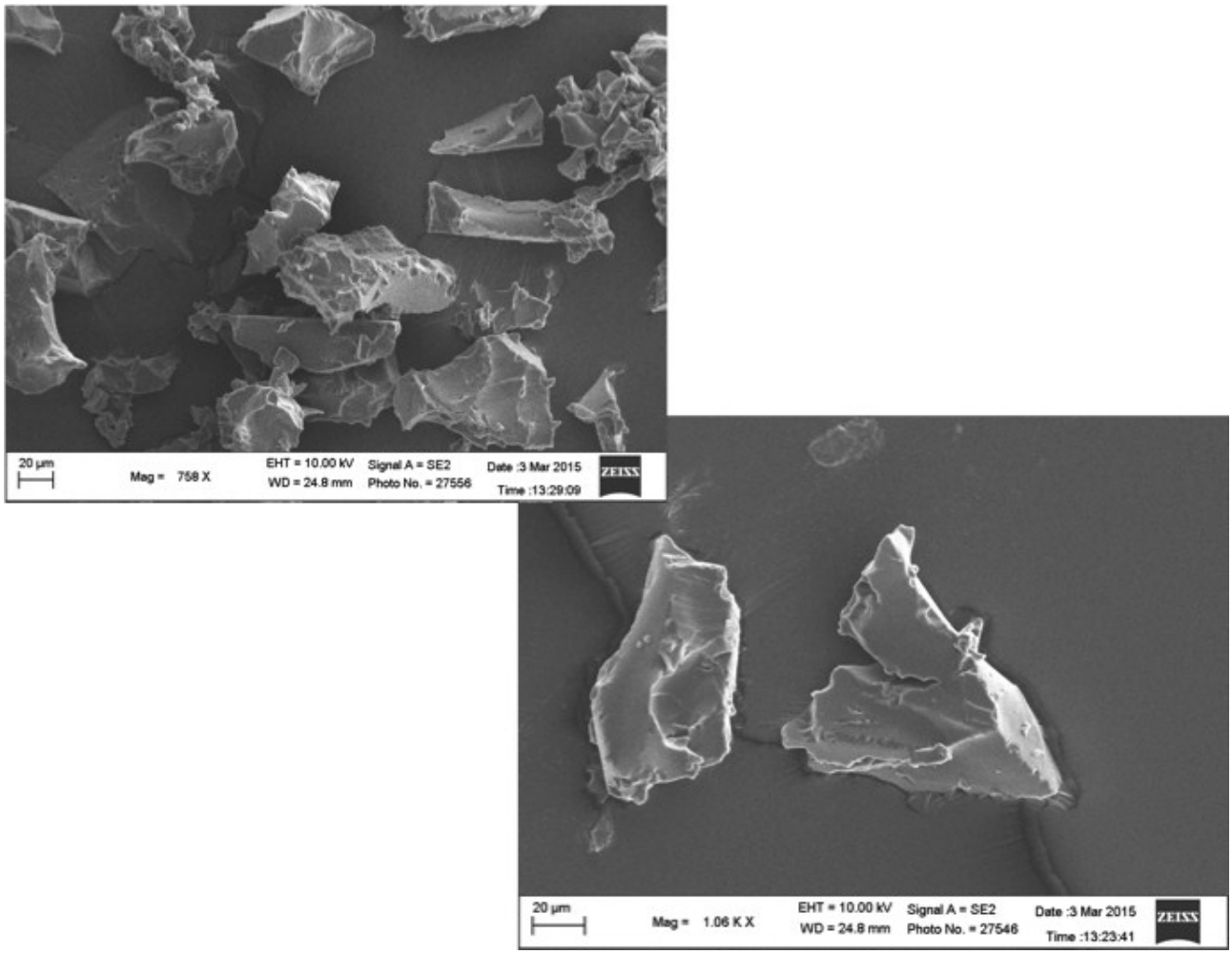


**Fig. S4:** SEM analysis of HyPPI gel particles

## LC-MS Characterization

a

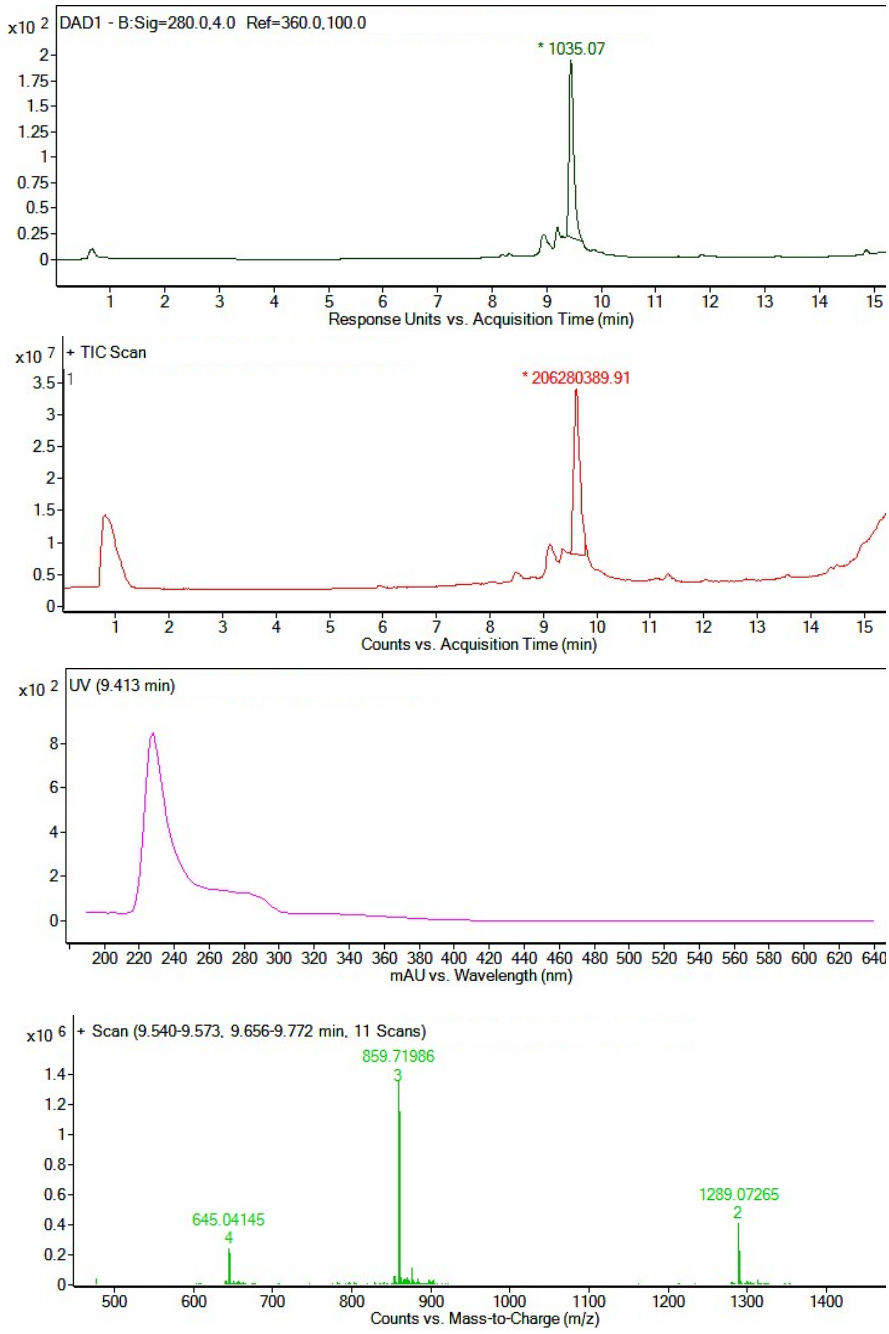


**Fig. S5a**: HPLC-MS characterization of purified AARE ($MW_{calculated}$=2578.38) peptide. The $[M/2]^{+2}$, $[M/3]^{+3}$ and $[M/4]^{+4}$ fragment ion peaks in the ESI scan spectra are indicated.

b

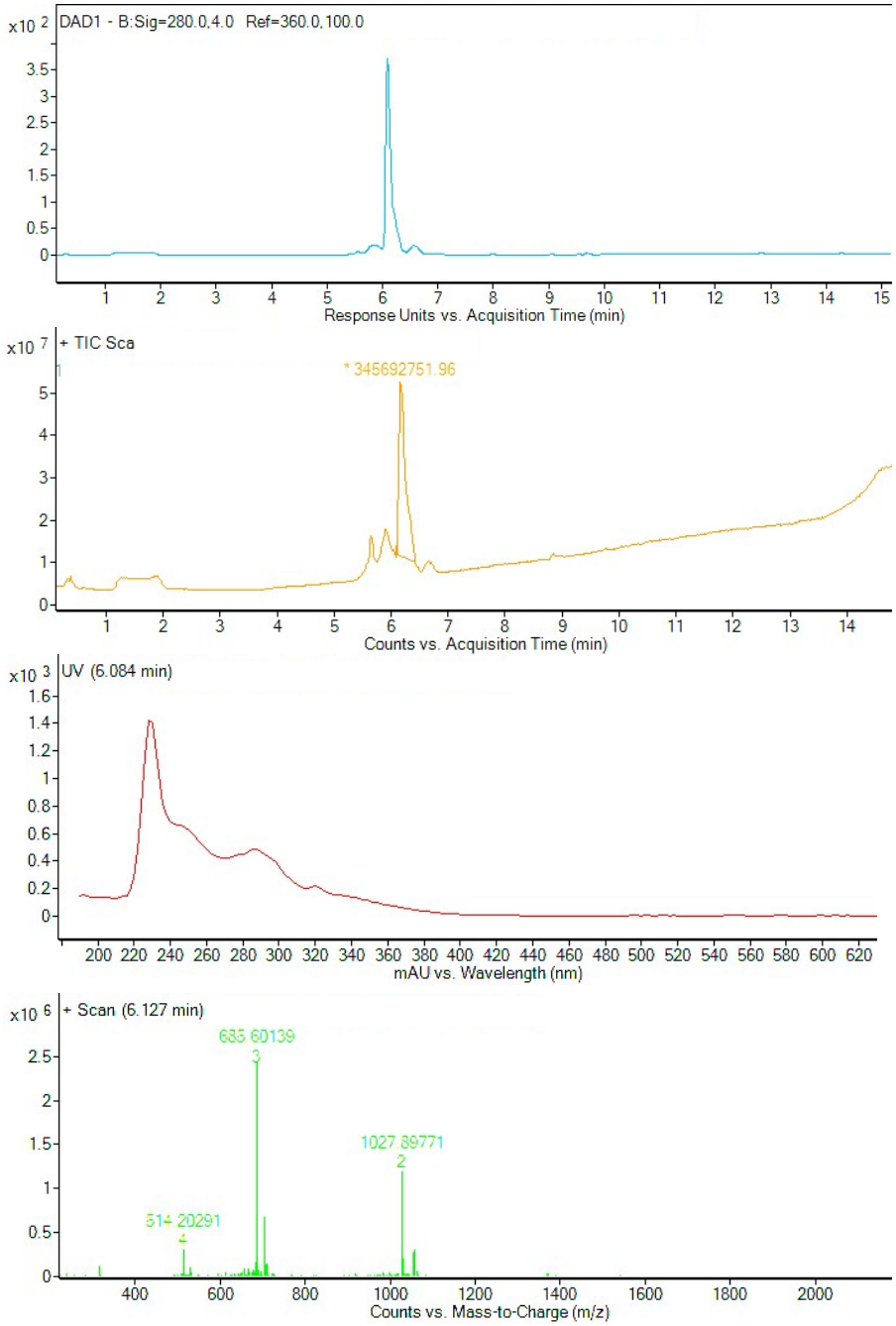


**Fig. S5b**: HPLC-MS characterization of purified n-AARE ($MW_{calculated}$=2053.64) peptide. The $[M/2]^{+2}$, $[M/3]^{+3}$ and $[M/4]^{+4}$ fragment ion peaks in the ESI scan spectra are indicated.

**NMR Characterization of AARE**

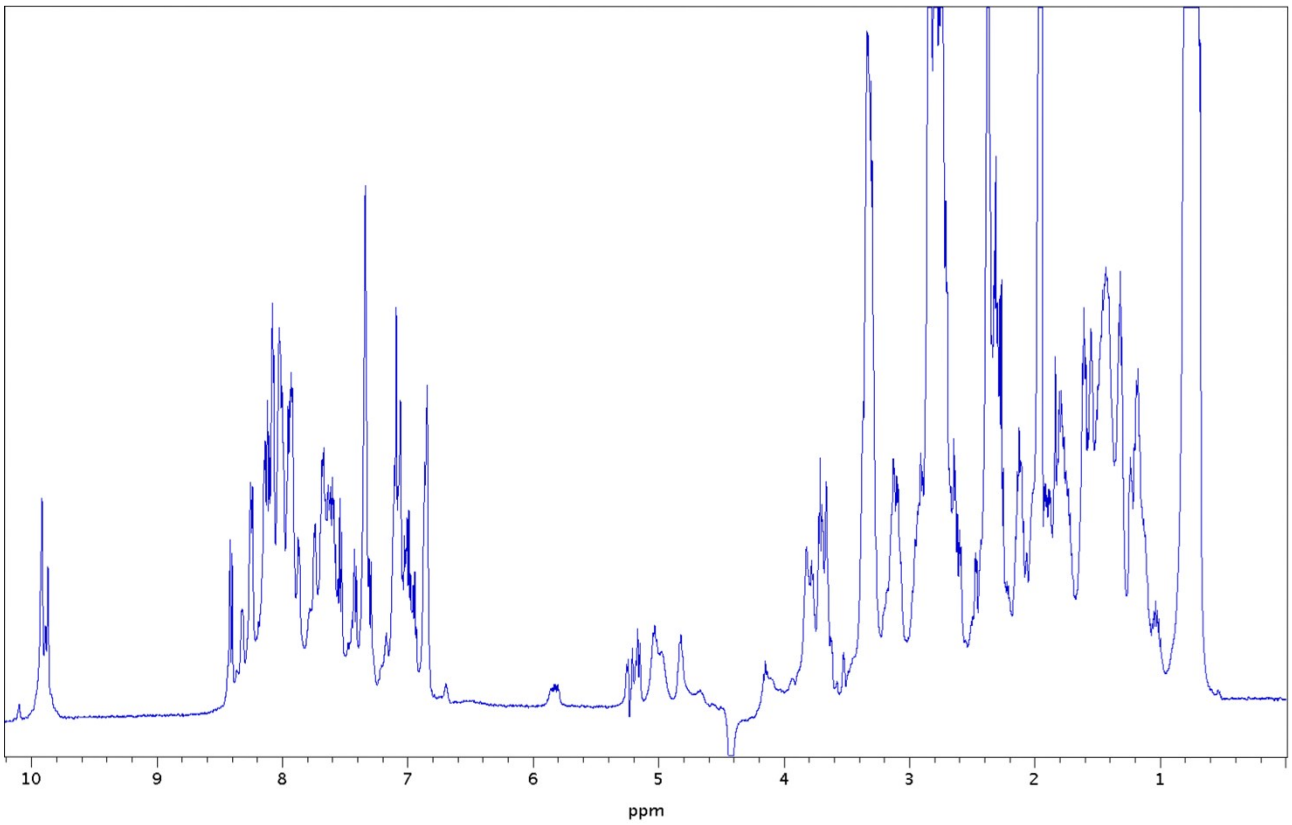


**Fig. S6a**: 1D $^{1}H$ NMR spectrum of AARE. Allylic protons, in the region between 5 ppm and 6 ppm, are shown.

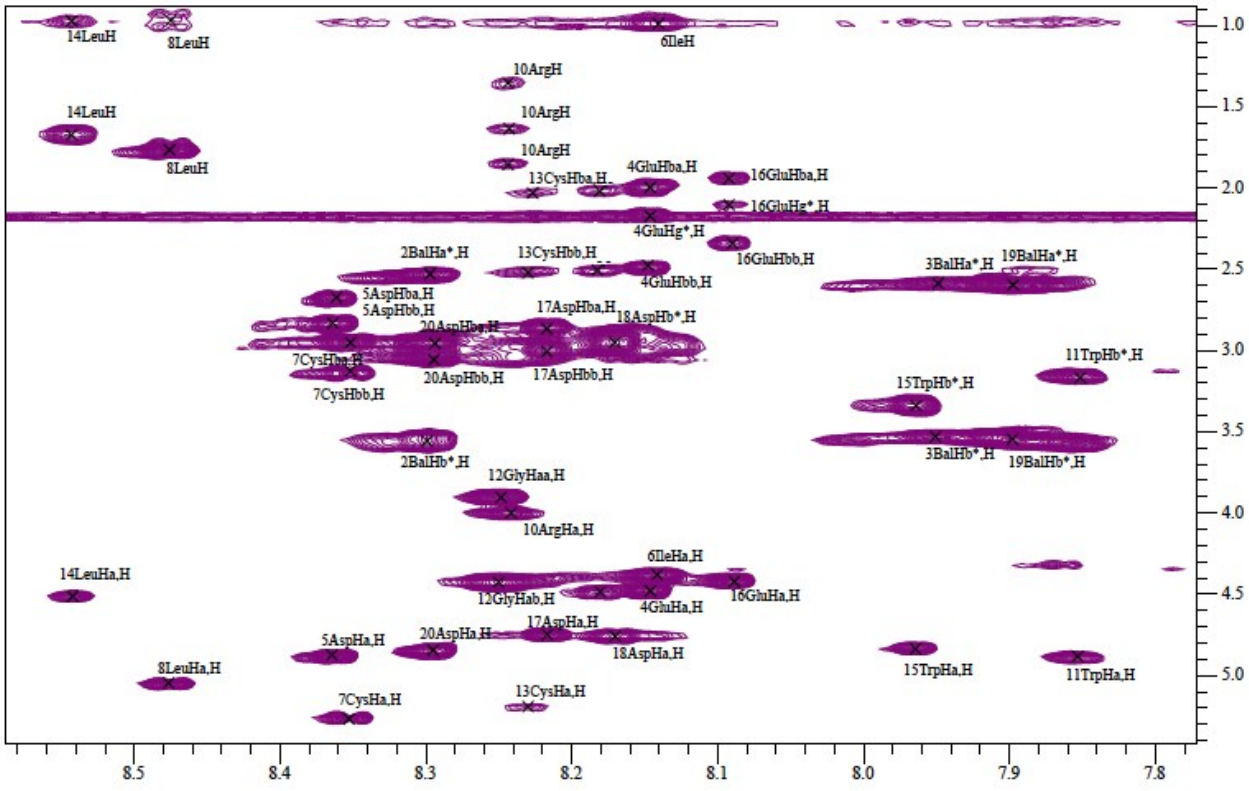


**Fig. S6b**: TOCSY spectrum of **AARE**. Assignment of peptide spin systems is shown.

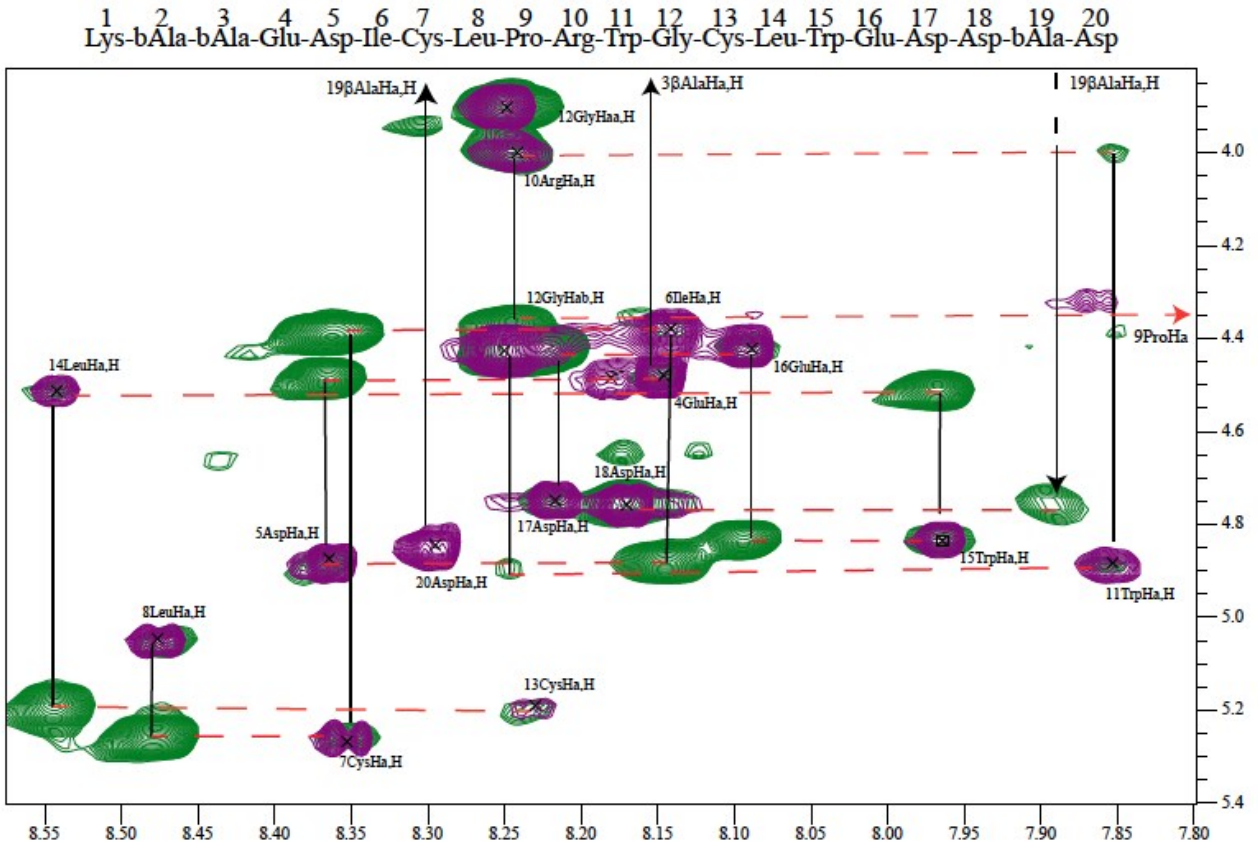


**Fig. S6c**: Superimposition of TOSCY (purple) and NOESY (green) spectra of AARE. Zoom of the region, where peaks of correlation between HN and Hα protons are present, is shown.
HN(i)-Hα (i-1) correlations are indicated by black and red lines. Vertical black lines symbolize the chemical shift of HN protons. Horizontal dashed red lines symbolize the chemical shift of Hα protons.

**Peptide/BSA affinity evaluation**

**ITC experiment**

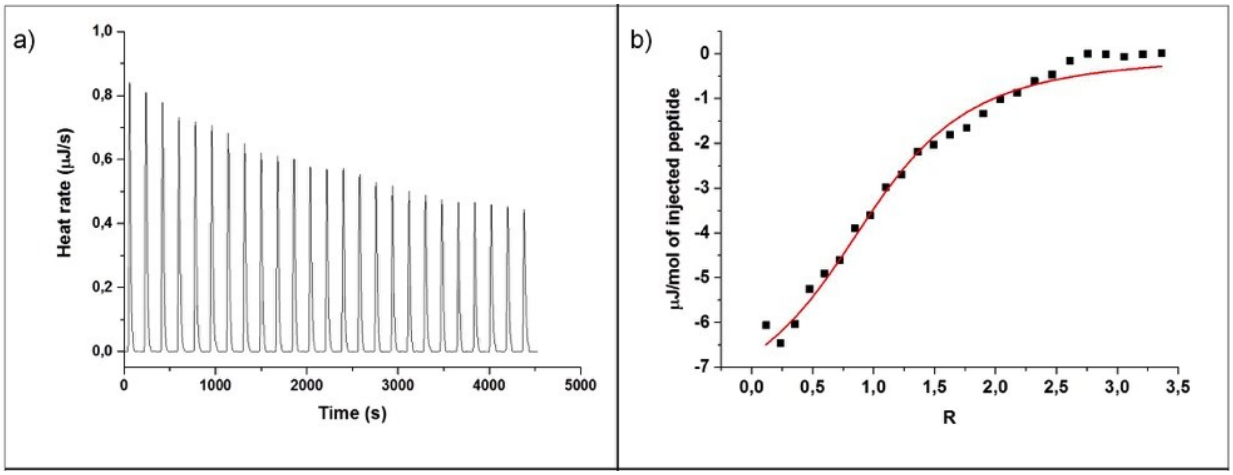


| | Ka ($M^{-1}$) | n | ΔH (kJ/mol) | $K_D$ (µM) | TΔS (kJ/mol) |
|---|---|---|---|---|---|
| **SAp** | **4.6 ± 3.3 E4** | **1.07** | **-7.955** | **21.7 ±3.3** | **18.6** |

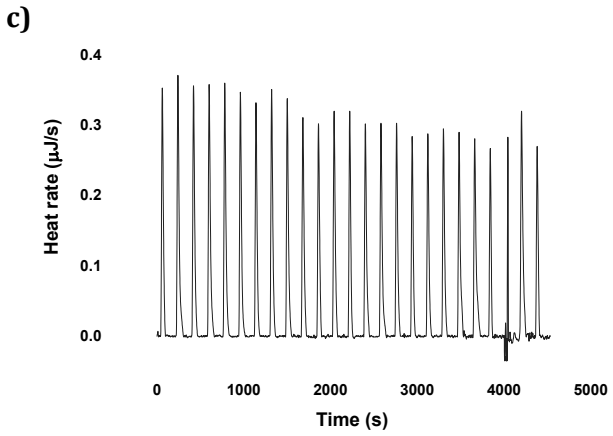


**Fig. S7:** ITC studies. On top (a and b) Calorimetric curve relative to BSA protein (0.1 mM) titration with SAp sequence (1 mM). Raw a) and integrated data b) are shown. In the table, the thermodynamic data were achieved with a fitting applying a single-binding-site model. c) Calorimetric curve for BSA protein (0.1 mM) titration with the unrelated sequence (1 mM).

**SPR experiment**

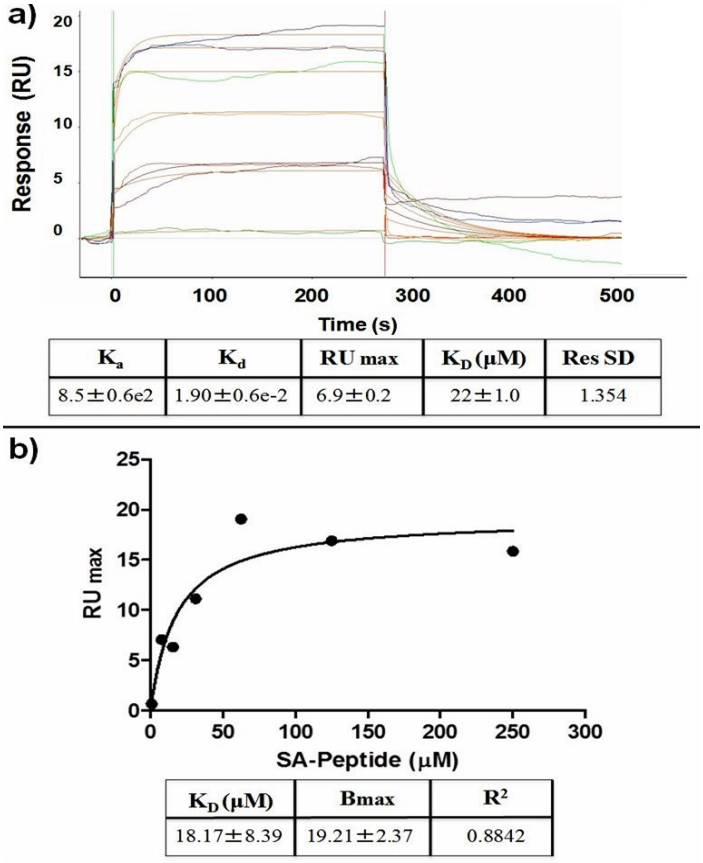


| $K_a$ | $K_d$ | RU max | $K_D$ (μM) | Res SD |
|---|---|---|---|---|
| 8.5±0.6e2 | 1.90±0.6e-2 | 6.9±0.2 | 22±1.0 | 1.354 |

| $K_D$ (μM) | Bmax | $R^2$ |
|---|---|---|
| 18.17±8.39 | 19.21±2.37 | 0.8842 |

**Fig. S8:** SPR data of SAp sequence, a) overlay of sensorgrams relative to the binding of SAp solutions to immobilized BSA channel; in the relative table, the kinetic parameters are reported; b) plot of RU signal from each experiment versus SAp concentration is shown.

**Fluorescence titration**

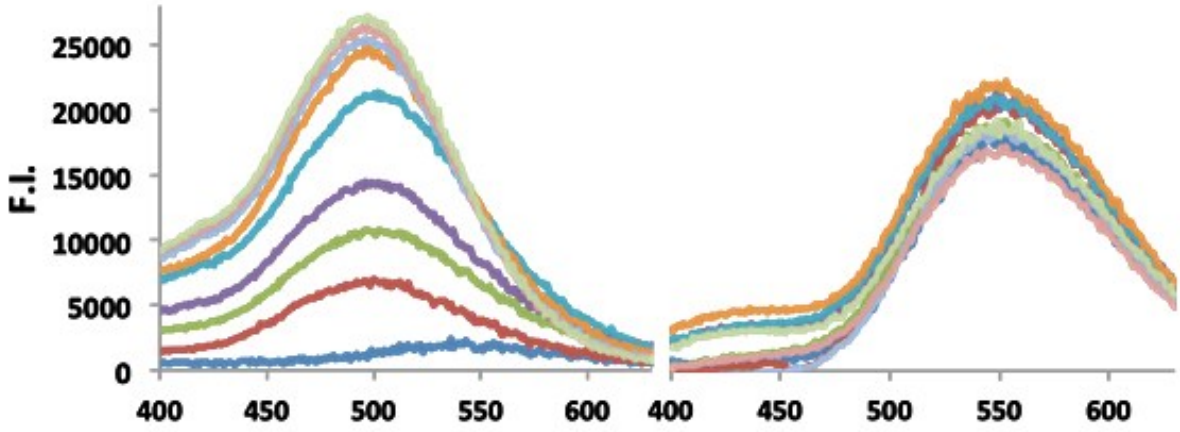


**Fig. S9**: The spectrophotometric titration of the AARE (left) and n-AARE (right) with the BSA solutions (ranging from 0 to 1.5 μM).

**TD-DFT Computational analysis of fluorescence**

The computed electronic excitation energies for the free dansyl molecule and the AARE show the same features, and contour plots of the frontier orbitals are very similar in both cases, the highest occupied molecular orbital (HOMO) and the lowest unoccupied molecular orbital (LUMO) are reported in Fig. 1b: these are involved in an important electronic transition characterized by an intramolecular charge transfer from the dimethylamino to the naphthalene sulphonyl groups. In details, the optical properties of a dansyl-peptide model system (see figure S9 for the details of its structure) have been computed in cyclohexane (ε = 2.02) and water (ε = 78.36) as representative of the local environments felt by the dansyl tag in presence and absence of the BSA protein, respectively and such behavior is maintained. More closely in both the solvents the electronic excitation corresponds to a HOMO-LUMO transition, characterized by a strong charge transfer degree from the dimethylamino group to the naphthalene sulphonyl moiety. The resulted twisted intra-molecular charge transfer (TICT) state is blue shifted in cyclohexane due to a major stabilization of the LUMO orbital in a more polar environment as the aqueous one. Moreover the shift computed by varying the solvent polarity is in quantitative agreement with that obtained from the spectrophotometric titration with the BSA protein. The increase of the fluorescence emission and the blue shift of the band are due to the change of the local dielectric constant felt by the dansyl group upon the formation of the BSA-peptide complex. In the case of the pure peptide in water solution, the dansyl tag is embedded in a high polar environment where non-radiative decay processes quench its fluorescence yield. The emission energy is computed at 523 nm (oscillator strength (f) = 0.149) in water solution in nice agreement with the experimental value of 540 nm detected for the pure specific peptide in water. Moreover in cyclohexane solution the emission is computed at 494 nm (f = 0.104) in quantitative accordance with the value measured after the addiction of the BSA protein. In both the solvents the electronic excitation shows an HOMO-LUMO character.

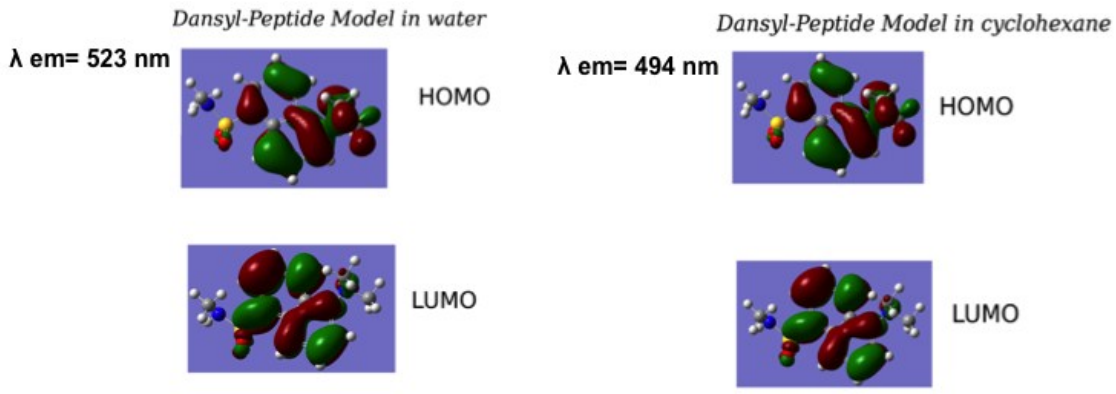


**Fig. S10:** Electronic states of Dansyl conjugated to the SAp in polar and apolar solvent.

A clear blue shift is observed in cyclohexane due to a major stabilization of the LUMO orbital in the polar environment. Moreover the shift computed by varying the solvent polarity is in quantitative agreement with that obtained from the spectrophotometric titration with the BSA protein.

Photophysical signatures (radiative lifetimes, radiative and non-radiative decay constants) were evaluated combining properties theoretically computed with experimental lifetimes, according to a general protocol recently formulated by some of us [6 7].

Shortly, the radiative decay constant (kr) is calculated according to:

$$k_r = \frac{4\ \Delta E^3}{3\ \ c^3}\mu 10^2$$

where ΔE is the emission energy computed at the excited state energy minimum structure, c is the speed of light and $\mu 10^2$ is the square root of the ground to the exited state dipole moment.

The radiative lifetime ($\tau_r$) is simply given by:

$$\tau_r = {}^1/k_r$$

Combining the computed kr with experimental lifetime ($\tau_{exp}$) is possible to obtain the non-radiative decay constant ($k_{nr}$):

$$k_{nr} = \frac{1}{\tau_{exp}} - \ k_r$$

We considered the experimental lifetimes for water and cyclohexane, whose respectively measured in absence and at the maximum concentration of the BSA protein.

Values of 0.0442 $ns^{-1}$ and 0.0254 $ns^{-1}$ for $k_{nr}$ were computed in water and cyclohexane, respectively, adopting the experimental lifetimes of the specific peptide in solution. In the same way values of 0.0326 and 0.025 $ns^{-1}$ are obtained for water and cyclohexane considering the lifetimes measured for the HydroMIP.

These data clearly suggest that non radiative decay constant and in turn non radiative decay pathways (whose nature is outside the purpose of the present paper) increase with the rise of the environment polarity leading to a strongly quenched fluorescence emission for the dansyl group in highly polar local environment.

**Selectivity studies on HyPPI polymers**

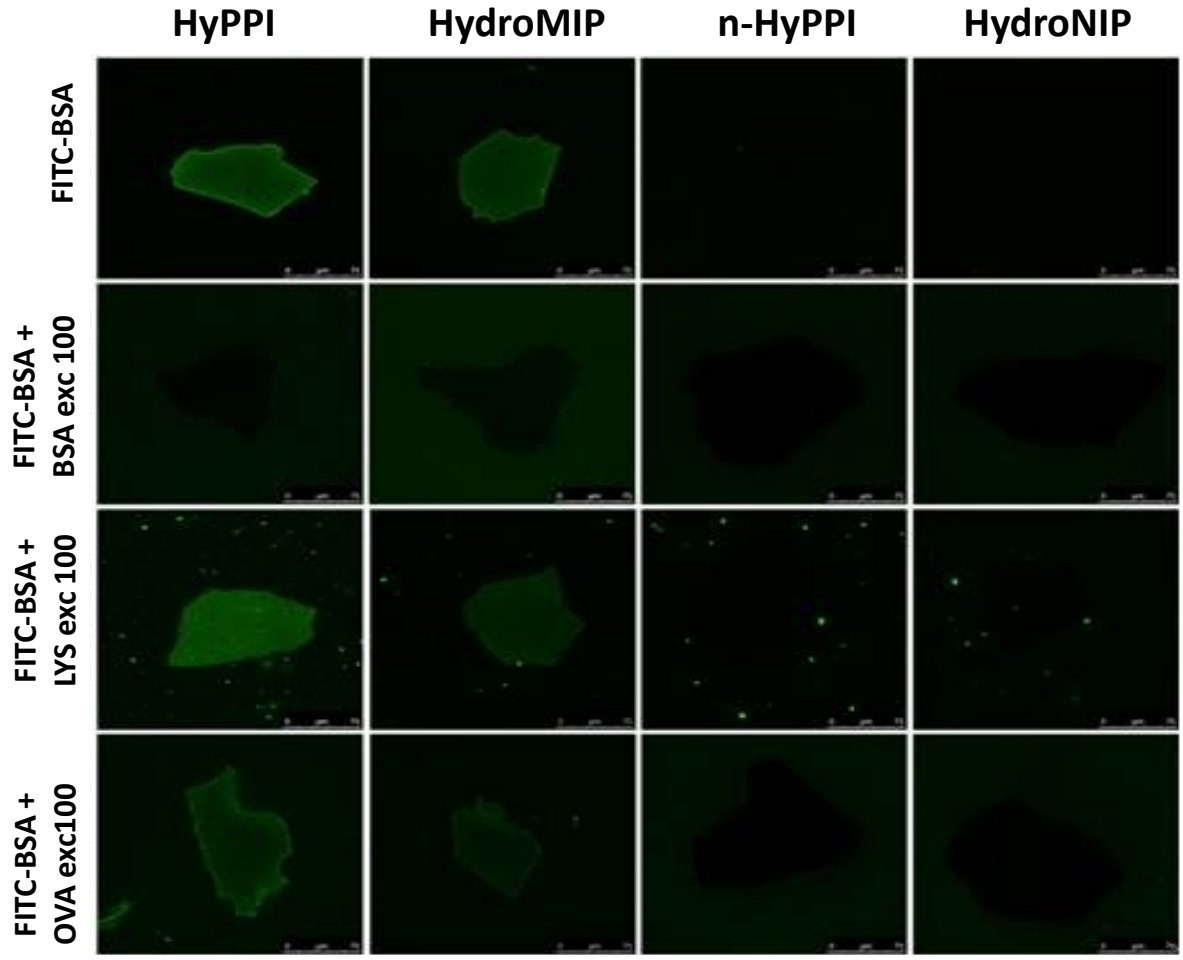


**Fig. S11:** Fluorescence microscopy images of competitive binding studies for HyPPI, n-HyPPI, HydroMIP and HydroNIP. A fix amount of FITC-BSA was added in presence of competitor proteins (BSA, lysozyme, and ovalbumin) at 100-fold molar excess**.**

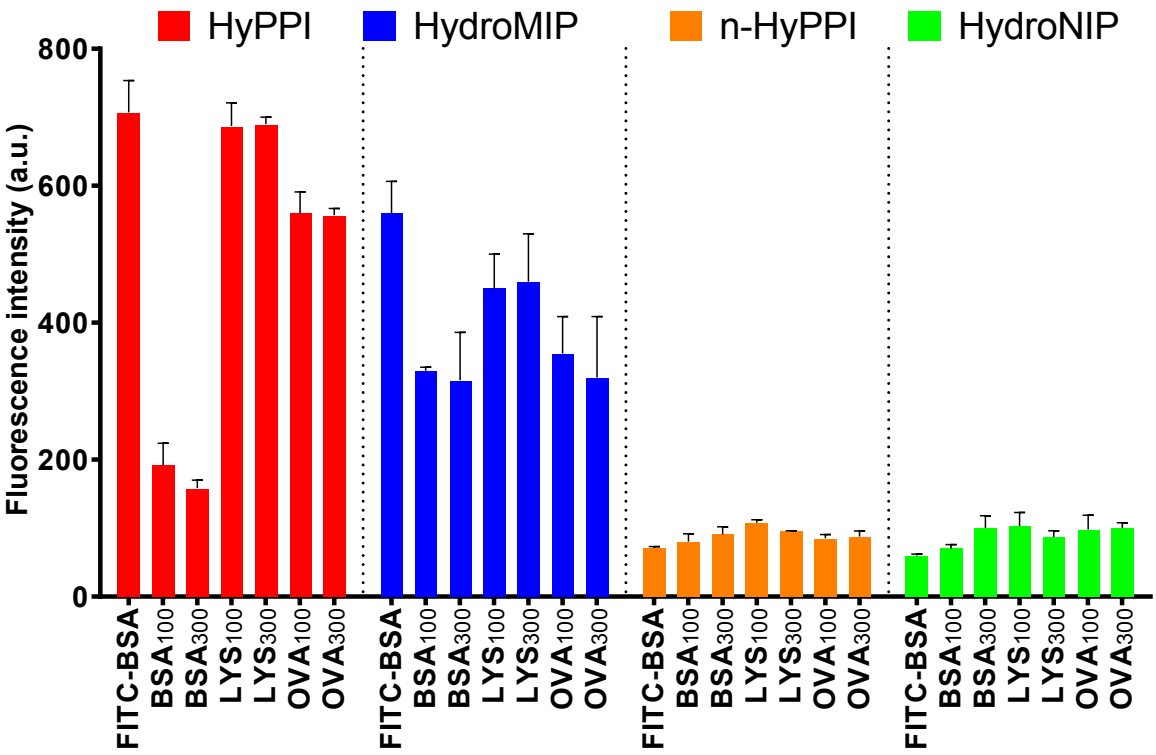


**Fig. S12:** Selectivity experiments by competitive assay for all materials synthesized.

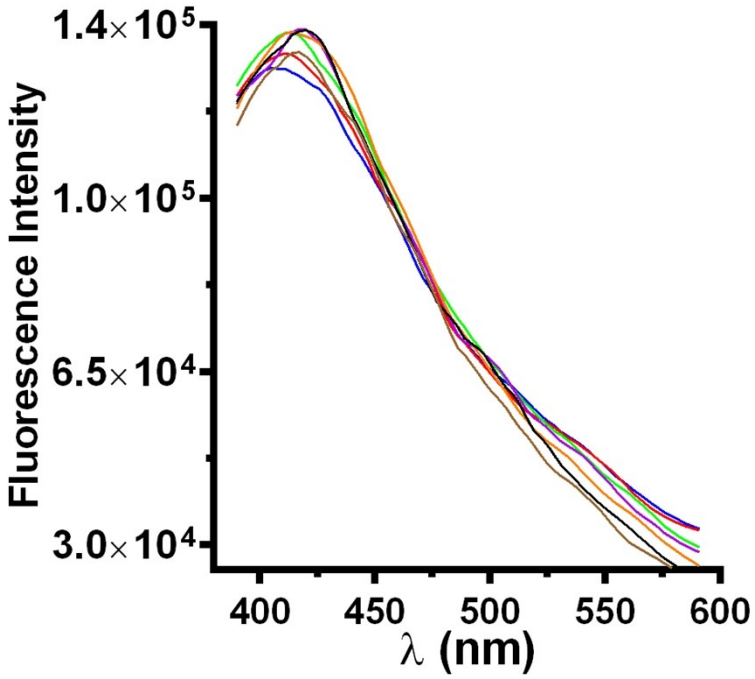


**Fig. S13:** Fluorescence emission of n-Dansyl-HyPPI (non-imprinted Hybrid dansyl-Peptide-Polymer) upon BSA titration.

## REFERENCES


1. Bergmann, N. M.; Peppas, N. A., Configurational Biomimetic Imprinting for Protein Recognition: Structural Characteristics of Recognitive Hydrogels. *Industrial & Engineering Chemistry Research* **2008,** *47* (23), 9099-9107.
2. El-Sharif, H. F.; Hawkins, D. M.; Stevenson, D.; Reddy, S. M., Determination of protein binding affinities within hydrogel-based molecularly imprinted polymers (HydroMIPs). *Phys. Chem. Chem. Phys.* **2014,** *16* (29), 15483.
3. El-Sharif, H. F.; Yapati, H.; Kalluru, S.; Reddy, S. M., Highly selective BSA imprinted polyacrylamide hydrogels facilitated by a metal-coding MIP approach. *Acta Biomater* **2015,** *28*, 121-7.
4. Baggiani, C.; Giovannoli, C.; Anfossi, L.; Passini, C.; Baravalle, P.; Giraudi, G., A Connection between the Binding Properties of Imprinted and Nonimprinted Polymers: A Change of Perspective in Molecular Imprinting. *J. Am. Chem. Soc.* **2012,** *134* (3), 1513-1518.
5. Dennis, M. S.; Zhang, M.; Meng, Y. G.; Kadkhodayan, M.; Kirchhofer, D.; Combs, D.; Damico, L. A., Albumin Binding as a General Strategy for Improving the Pharmacokinetics of Proteins. *Journal of Biological Chemistry* **2002,** *277* (38), 35035-35043.
6. Savarese, M.; Aliberti, A.; De Santo, I.; Battista, E.; Causa, F.; Netti, P. A.; Rega, N., Fluorescence Lifetimes and Quantum Yields of Rhodamine Derivatives: New Insights from Theory and Experiment. *The Journal of Physical Chemistry A* **2012,** *116* (28), 7491-7497.
7. Savarese, M.; Raucci, U.; Netti, P. A.; Adamo, C.; Ciofini, I.; Rega, N., Modeling of charge transfer processes to understand photophysical signatures: The case of Rhodamine 110. *Chem. Phys. Lett.* **2014,** *610-611*, 148-152.